Application of fiber element in the assessment of the cyclic loading behavior of RC columns

R. Sadjadi[†] and M.R. Kianoush[‡]

Department of Civil Engineering, Ryerson University, Toronto, Ontario, Canada

Abstract. This paper studies the reliability of an analytical tool for predicting the lateral load-deformation response of RC columns while subjected to lateral cyclic displacements and axial load. The analytical tool in this study is based on a fiber element model implemented into the program DRAIN-2DX (fiber element). The response of RC column under cyclic displacement is defined by the behavior of concrete, and reinforcing steel under general reversed-cyclic loading. A tri-linear stress-strain relationship for the cyclic behavior of steel is proposed and the improvement in the analytical results is studied. This study only considers the behavior of columns with flexural dominant mode of failure. It is concluded that with the implementation of appropriate constitutive material models, the described analytical tools can predict the response of the columns with reasonable accuracy when compared to experimental data.

Keywords: reinforced concrete; cyclic loading; analytical; fiber element; column; non-linear; constitutive model.

1. Introduction

In reinforced concrete (RC) structures, columns are the most important elements in terms of maintaining the stability of the structure. Therefore failure of the column in the event of an earthquake is of main concern. The seismic performance and the capacity assessment of RC columns are usually performed in the form of the lateral load-lateral displacement relationship.

Due to complex interaction between the various components of real structures, their dynamic characteristics up to failure cannot be identified solely from dynamic tests of scale models. Moreover, the cost of such tests for large specimens is substantial. Historically these difficulties have been overcome by static tests on components and on reduced scale sub-assemblages of structures under cyclic load reversals. Results from these tests are then used in the development of hysteretic models that permits the extrapolation of the available test data to other cases and to the dynamic response of the complete structures (Taucer 1991). Based on earthquake resistant design philosophy, the seismic energy input should be dissipated through largest possible number of inelastic regions within the structure. To avoid the formation of a side-sway collapse mechanism, columns are expected to remain elastic during the earthquake response, except at the base of the

---

† Graduate Research Assistant, E-mail: rsadjadi@ryerson.ca
‡ Professor, Corresponding author, E-mail: kianoush@ryerson.ca

building where hinging is desired. Attention is thus focused on predicting the seismic behavior of first story columns including their energy dissipation capacity. Behavior of reinforced concrete columns has been the subject of many investigations. These researches may be divided into three main categories (Esmaeily 1999). The first category includes those studying the effect of amount, size and arrangement of reinforcement. The second category includes all the investigations regarding the material properties, such as the strengths of concrete. The third category includes all the research, in which different loading conditions such as the effect of variable axial load is investigated which is also the subject of investigation in this paper.

2. Analytical models

There are two major categories for the nonlinear dynamic analysis of reinforced concrete structures. One is to present the overall behavior of each structural component in terms of a macro-model. These models are based on approximations of the physical behavior of RC members and have been widely used for investigation of the response of multistory buildings because of their simplicity. However the accuracy of these models is questionable as there is no true representation of the controlling parameters in their nonlinear behavior. The second option, namely micro-model, is to discretize each structural component into smaller units and then capture the overall behavior of the component in terms of the behavior of those smaller units. Although micro-models including fiber element models, are more accurate based on the degree of their complexity, but their implementation in dynamic response analyses of large structures can be prohibitively expensive. Fiber element technique has become one of the most popular and promising method of analysis of RC sections and has been used extensively in numerous researches involving the analysis of cyclic behavior of concrete columns (Golafshani et al. 2002, Dhakal 2006, Bechtoula et al. 2009).

In fiber element model, it is assumed that the plastic hinges form in the members' ends and parts of the length of the element can experience inelastic deformations. The fiber model corresponds to a large level of discretization, where each structural member is modeled as a single element and the stress-strain relationships for steel and concrete are evaluated during the analysis of several cross-sections comprising the element. The fiber model has the ability to represent the behavior of the reinforced concrete members particularly in the critical regions of the element as concrete material type, volume, and spacing of reinforcement could vary along the member length. In fiber model, the element is divided into a discrete number of cross sections (segments). The model assumes constant fiber properties over each segment length, based on the properties of the monitored slice at the center of each segment. The non-linear behavior of the element is monitored at these control sections, which are in turn discretized into longitudinal fibers of plane concrete and reinforcing steel as is shown in Fig. 1. The non-linear behavior of the section is then captured from the integration of the non-linear stress-strain relationship of the fibers. This feature permits the modeling of any type of structural element including columns with different material properties in the cross-section.

"For RC columns, it is convenient to work with the member axis and the perpendicular cross-section. The stress resultants over a cross-section can be categorized as normal and shear stresses and the total deformation can be classified into flexural and shear deformations for reduced three-dimensional stress states. Flexural deformation results from normal stresses and can be computed on the basis of the Euler-Kirchhoff hypothesis (in-plane theory). Shear stresses cause additional shear deformation, which can be evaluated by relaxing the Euler-Bernoulli assumption so that the cross-
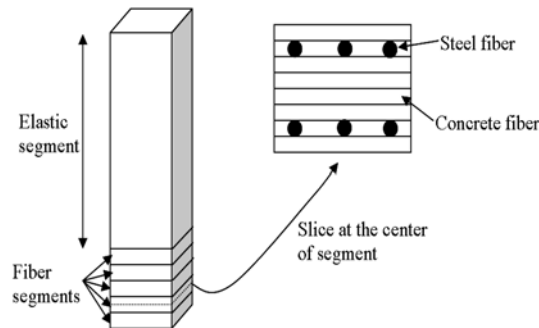
Fig. 1 Depiction of segments and fibers

section is not necessarily normal to the member axis after deformation but still remains a plane (Maekawa *et al.* 2003). The validity of this assumption has been confirmed for RC frame members whose member length is long compared with the dimension of cross-section (Furlong 1979), (Ramamurthy 1966). For slender RC members flexural action tends to govern the overall behavior while the effect of shear is relatively small, therefore accurate modeling of the flexural behavior is the key to the accurate prediction of the overall behavior of the member" (Maekawa *et al.* 2003). In the fiber model the formulation is based on the assumption of complete bond between all fibers, therefore, phenomenon such as shear failure, bond deterioration between steel and concrete can not be explicitly modeled and such effects are not covered in this study. The present study is based on fiber formulation concept which is implemented in the computer program DRAIN-2DX (fiber element). The element is assumed to be elastic in shear. This paper is focused on the investigation of the columns with flexure dominant mode of failure.

3. Plastic hinge zone

It is expected that the bases of all columns in the first story experience plastic hinging. As the column experiences cyclic displacement, plastic deformation spreads into the member which should be captured for the simulation of the inelastic behavior of the RC member. In reinforced concrete columns, the equivalent plastic hinge length is determined based on the experimental curvature distribution and deflection. Therefore the effect of longitudinal reinforcement yield penetration and the cracking due to shear are included in the equivalent plastic hinge length (Sakai and Sheikh 1989). In fiber element model, material nonlinearity can spread over a finite length of the element which is considered as plastic hinge and is modeled by a fiber section; whereas the rest of the element length is modeled as an elastic section. There are different suggested values for the length of the plastic hinge ranging from 0.5 h to h, where h is the member's depth. Sakai and Sheikh (1989) pointed out the influence of the increase in axial load level, amount of transverse reinforcement, and aspect ratio (height to side ratio) of the column on the increase in plastic hinge length. Bae and Bayrak (2004) studied the influence of the plastic hinge length on the relationship between ductility parameters and concluded that the reduction of plastic hinge length from h to 0.5 h although reduced the displacement ductility values, but did not have a significant influence on the relationship between the various ductility parameters. The length of the plastic hinge used in this paper for the calculation of the fiber segment length in RC columns is as suggested by Paulay and
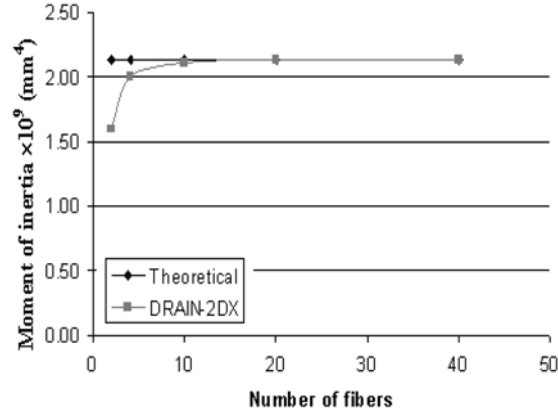
Fig. 2 Effect of number of fibers on moment of inertia of the cross-section

Priestly (1992) and calculated as

$$l_p = 0.08l + 0.022d_b \times f_y \qquad (1)$$

where l is the total length of the element, d_b is the longitudinal bar diameter, and f_y is the yield stress of steel. This equation is based on the tests on circular, square, and square hollow columns.

4. Effect of the number of fibers in the cross-section

Regardless of the high memory demand and increasing computational cost, the accuracy of the model increases with the number of fibers in each cross section. Although DRAIN-2DX requires a minimum of two fibers for modeling a cross section, there are no upper limits specified for the number of fibers in the cross section or the number of segments for modeling a member. It is possible to specify a large number of fibers for analysis of a model consisting of one or two elements. However, discritization of the cross section into a large number of fibers might not be practical for the analysis of large models with several elements. Although the large number of fibers increases the accuracy and also the execution time, there must be a compromise between accuracy and time of execution. For a better understanding of the problem with accuracy, the results of analysis of a rectangular section moment of inertia (I) with different number of fibers are compared to the calculated value obtained using the equation, $I = b \times h^3/12$ (for a rectangular section with $b = h = 400$ mm, $I = 2.133$ E^9 mm^4). Fig. 2 shows the results of the analysis of the same section with different number of fibers in the cross section (slice). The theoretical value for moment of inertia, is shown by a horizontal line. It is observed that for the number of fibers of more that 20 which is used as a lower limit in this research, there is a negligible difference between the analytical values obtained from DRAIN-2DX, and the theoretical value of the moment of inertia. For a smaller number of fibers, the results may become less accurate.

5. Material models

For members with flexural dominant mode of behavior, the three-dimensional strain field

developed in the frame member can be decomposed into a one-dimensional one over the cross-section (Maekawa *et al.* 2003). With accepted level of accuracy, the three dimensional behavior of concrete and steel can be simplified into uniaxial stress-strain relationship. Because the nonlinear behavior of the fiber element derives entirely from the nonlinear behavior of the constituent material fibers, the validity of the analytical results depends on the accuracy of the uniaxial stress-strain relationship curves for concrete and steel. The effect of concrete confinement by reinforcement is considered by using appropriate uniaxial monotonic envelope of concrete which incorporates such effect including arrangement and mechanical properties of the transverse reinforcement. This is of great importance since it is assumed that the concrete monotonic stress-strain curve represents the envelope for the cyclic stress strain branches. A study by Lokuge *et al.* (2004) concluded that the monotonic loading curve serves as the envelope for the hysteretic response for unconfined and confined normal strength concrete. For high strength concrete this assumption is valid only for the ascending branch. The material model for concrete in DRAIN-2DX considers cracking and crushing and tension stiffening. The concrete material properties are defined as points in the stress-strain curve shown in Fig. 3. There is a maximum of five points for defining the stress-strain relationship in compression, and two points for defining the stress-strain relationship in tension. The point with coordinates (σ_{1C}, ε_{1C}) refers to the cracking of the concrete and the point (σ_{2C}, ε_{2C}) refers to the maximum compression strength of the concrete. The point (σ_{3C}, ε_{3C}) defines the ultimate strength of concrete under high strains. The horizontal branch shows the ability of concrete to sustain some strength at very large strains. The slope of descending branch which is highly dependent on the confinement condition of the cross section has a significant effect on the ductility of the element during cyclic loading demanding an accurate material model for the concrete incorporating the volume, arrangement, and properties of transverse reinforcement. Several models have been proposed for the stress-strain relationship envelope for concrete in compression with consideration of the effect of the confinement. Except Case study 2 presented later in this paper where the values proposed by the researchers were implemented in the analysis, the model proposed by Hoshikuma *et al.* (1997) is selected for defining the material model for core concrete for both circular and rectangular sections. The model is basically proposed for confined reinforced concrete in bridge piers considering different mechanical properties, configuration and volumetric ratio of the hoops and cross ties. The model has the advantage of yielding very comparable results for tests with a wide range of volumetric steel ratios ranging from 0.19 to 4.66%. The models proposed by Kent and Park (1971), and Mander (1988) are selected to represent the behavior of the unconfined
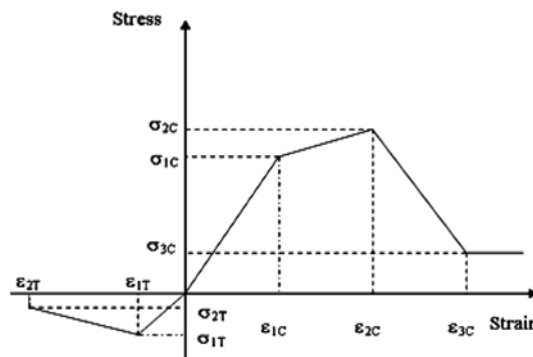

Fig. 3 Material model for concrete in DRAIN-2DX

concrete in the cover concrete for rectangular and circular sections, respectively. The relationship developed by Vebo and Gali (1977) has been adopted to represent the effect of concrete in tension under cyclic loading. The definition of tension softening behavior of the concrete is mesh size dependent (Lu *et al.* 2006, Roesler *et al.* 2007, Kwon *et al.* 2008).

Shima and Okamura (1987) proposed a model for tensile behavior of concrete after cracking which is expressed as the explicit relation between average stress and average strain as shown by

$$\sigma = f_t \cdot \left(\frac{\varepsilon_{tu}}{\varepsilon}\right)^c \qquad (2)$$

where σ is the average tensile stress, ε is the average tensile strain, f_t it is uniaxial tensile strength, ε_{tu} is cracking strain and c is a stiffening parameter. For plain concrete, the formulation of the average stress-average strain relation is dependent on the element size to maintain the same energy release. Parameter c is dependent on the size of the element and therefore, the resulting average tensile stress-strain relation depends on the element size. Through the appropriate determination of parameter c, the envelope of post-cracking tensile stress defined by Eq. (2) is applicable to both plain concrete and RC. For a seismic analysis the imperfection of the above equation does not matter since the strain level concerned is beyond the yield point. The model was verified to be independent of element size and orientation of the reinforcement in the element (Maekawa *et al.* 2003).

An empirical formula obtained by a trial and error process was also proposed by Shayanfar *et al.* (1997) which gives an appropriate value of ultimate tensile strain as a function of the element size so that the energy dissipation capacity and the ultimate load of the structure remain constant irrespective of the size of the element used in the mathematical model.

One of the advantages of the fiber element model as described in this paper lies in its simplicity and convenience in defining the tensile properties of the concrete material. A sensitivity study was performed and it was observed that the rate of softening has a very negligible effect on the post yielding response during high levels of strains experienced during the load reversals. This avoids significant complexity as normally encountered when defining the mesh size dependent tensile properties of concrete in a finite element analysis.

In the sensitivity study on the column introduced as Case-1 in this paper, the ultimate tensile strain values of concrete were arbitrarily changed to 5 and 10 times that of the actual values used. It was observed that after the second level of drift, the responses become almost identical.
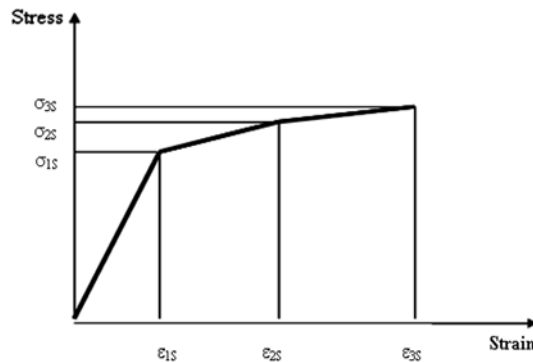

Fig. 4 Material model for steel in DRAIN-2DX

The material model for steel bars in DRAIN-2DX is shown in Fig. 4. The program assumes that the steel behavior is identical in tension and compression. As depicted in Fig. 4, DRAIN-2DX steel model assumes the steel modulus in different stages to reduce consequently. Thus, it is not possible to model the yield plateau behavior after yielding of the steel as it has a lower modulus than the ensuing strain hardening state. Several models have been proposed for defining the stress-strain relationship for steel. These models range from a simple elasto-plastic idealization to more complex models such as that proposed by Menegotto and Pinto (1973) for the steel. In this study it is aimed to propose a simple model to satisfy the requirements of the DRAIN-2DX material model while incorporating essential characteristic of the cyclic behavior of steel.

Bauschinger (1887) reported that the modulus of elasticity of steel reduces at subsequent cycles after the steel has been strained beyond the elastic limit. The analysis of the test data has confirmed that the unloading modulus decreases, and that the rate of decrease is especially rapid after yielding but stabilizes at larger strains. Dodd and Restrepo-Posada (1995) proposed a relationship between the maximum plastic strain and the unloading modulus of steel as

$$E_u = E_s\left[0.82 + \frac{1}{5.5 + 1000\,\varepsilon'_M}\right] \tag{3}$$

E_u, E_s, and ε'_M are the unloading modulus of elasticity, the initial modulus of elasticity, and the maximum plastic strain, respectively. When reversed cyclic loading is applied to a steel bar, stress-strain curve becomes nonlinear at a stress lower than the initial yield strength. This phenomenon is known as Bauschinger effect. Mander (1983) has proposed a softened branch depicted in Fig. 5 to simulate this effect on the stress reversals. This is an important aspect in the cyclic behavior of the steel which should be considered in modeling the behavior of the element under load reversals. To add all the aforementioned effects to the fiber model in DRAIN-2DX, a tri-linear approximation of the cyclic behavior curve is introduced as illustrated in Fig. 6. The coordinates of this tri-linear approximation in terms of the stress and strain values are also shown in the same figure as a function of mechanical properties of steel and the reduced modulus of elasticity (E_u) as obtained from Eq. (2) for each level of drift. When a steel fiber has experienced plastic deformation, the bi-linear stress-strain relationship is replaced by the proposed tri-linear approximation, where yield stress of f_y is reduced by a factor ranging between 0.8 to 0.9, corresponding to a higher strain than conventional value of around 0.002. The second part of the tri-linear curve connects the yield point to a point determined by stress value ranging between $1.05f_y$ to $1.10f_y$, and a strain value which is a
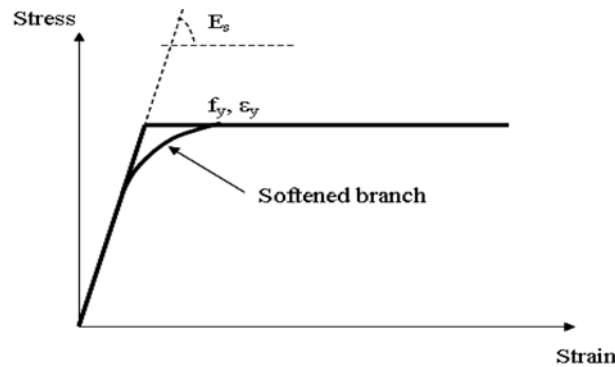

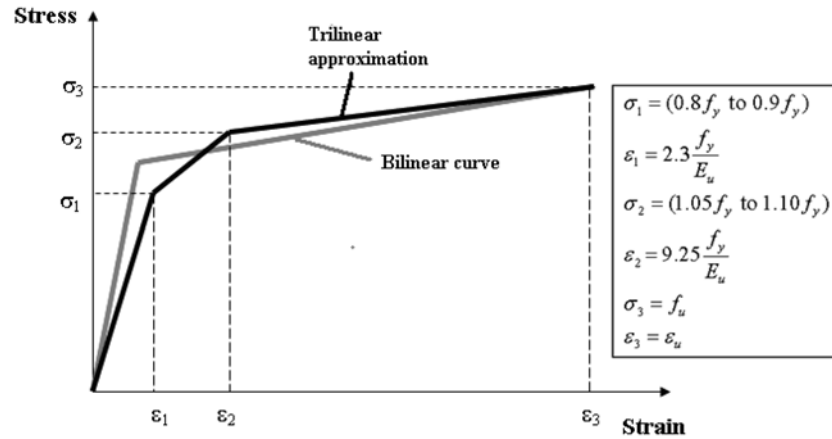Fig. 5 The softened branch in the stress-strain behavior of steel

Fig. 6 The proposed tri-linear material behavior for steel

function of reduced modulus of elasticity and maximum strain experienced by steel. This model will ensure that the effect of stiffness degradation of steel is considered in the analysis and the hysteretic response of steel is more realistically represented. The model is based on the fact that each layer of steel has experienced the maximum strain associated with the previous cycle's maximum drift, therefore its modulus of elasticity is reduced based on the maximum level of strain experienced in that cycle which is obtained by using Eq. (2). For obtaining the required analytical curve of the experiment, several complete analyses are performed with the complete loading history of the test, where each complete analysis has a certain tri-linear properties such as the reduced modulus of elasticity of steel for that stage of analysis. The desired complete load-deformation response consists of several load-deformation loops; one for each cycle (i.e., level of drift) that is selected from the corresponding analysis, using appropriate tri-linear properties for that level of drift and is then added to the total load-deformation history. For implementation of the proposed model, the analysis is divided into different stages based on maximum steel strain at each level of drift of the RC column, the associated reduced modulus of elasticity, and its tri-linear properties for each layer of steel in the cross section. First, a complete analysis of the entire loading history is performed using bi-linear properties for all steel fibers that are located in different elevations in the cross section. Based on the maximum strains in the top-most and bottom-most fibers of the cross-section at the end of each level of drift (obtained from the output data), the maximum strain in each layer of steel fiber is calculated using linear strain relationship in the section. The tri-linear approximation, using corresponding reduced modulus of elasticity, will replace the bilinear relationship wherever the steel layer has yielded. Then another complete analysis is performed for that certain level of drift using updated steel properties. After completion of this analysis, the loop corresponding to that certain level of drift will be selected from force-deformation curve and will form a part of the final analytical result, corresponding to that certain level of drift. The same procedure is done for next levels of drift and the data for each level of drift will form parts the final analytical curve.

5.1 Pullout of reinforcing bars from the footing

At low axial loads, bar slip appears to account for approximately half of the total deformation at

yield and can have a major effect on reduction of the effective flexural stiffness of a column (Elwood and Eberhard 2006). This is of more concern for small size elements. Elwood and Moehle (2003) proposed a relationship for calculation of the yield displacement due to bar slip at yield based on parameters such as the diameter of the bar, stress in the tension reinforcement, and the average bond stress between the longitudinal reinforcement and the footing concrete.

Because of the fact that fiber element formulation assumes that there is no debonding between the concrete and steel, this effect could not be explicitly modeled.

In the current paper the effect of bond slip on the reduction of the effective flexural stiffness of column is approximated by the reduced stiffness of the steel in the proposed trilinear model. The trilinear model appears to capture the post yielding behavior of the column, including the pull out effect, with reasonable accuracy.

5.2 Buckling and rupture of rebars

In this study, it is not intended to address the buckling and rupturing loads of the columns' longitudinal reinforcement, but rather to check the ability of the model to simulate the behavior using experimental results. Theoretical foundation for the buckling load determination in reinforced concrete columns is beyond the scope of the current paper and can be found elsewhere (Krauberger *et al.* 2007).

An approach similar to the one suggested by Lee and Pan (2001) is adopted here for modeling the buckling of reinforcement bars. Accordingly, a very small value for the modulus of elasticity is defined when the stress in the longitudinal steel exceeds the buckling stress of the rebar as reported in the experiment. For implementation in the tri-linear model, the strain in the buckled rebar is calculated based on the maximum strains in the end fibers of the section, strain gradient and its distance to the end fiber, using the experimental observation including the maximum drift at the occurrence of buckling. A complete analysis will be performed using the modified stress-strain relationship for the buckled steel. The loops corresponding to force-displacement cycles after buckling is selected from this analysis and attached to the end of the previous data of pre-buckling cycles. For simulating the rupture of the rebars, the corresponding steel fibers are removed from the cross section fibers for remaining loading history after rupture is reported in experimental test. The detailed description of the above-mentioned procedure is presented later for Case-study 3 where the RC column experienced buckling and rupturing of rebars during the last deformation cycles. The tri-linear model is able to provide more realistic representation of the cyclic behavior of RC columns including the dissipated energy as can be observed from comparison of analytical and experimental force deformation curves presented later in this study. To observe the improvement of such modeling, analytical results are compared to those of the cyclic loading test of several experiments. Three case studies with different variables including cross-sectional dimensions, axial load condition and rebar configuration are presented in the next sections. To reduce the memory demand in the analysis when the specimens were subjected to repeated cycles of equal displacements, only one cycle per each level of drift is performed. When a deflection reversal is repeated at the same attained maximum amplitude the loading stiffness in the second cycle is expected to be lower than that in the first cycle, but the resistances at the peak displacement are similar (Otani 1980). Therefore it is reasonable to perform one cycle per each level of drift in the fiber element analysis for such a simulation.

5.3 Case-study 1

The result of an experiment conducted by Park (1990) on a rectangular cantilever column is used for evaluation of the fiber model analysis. The RC column has a height of 1784 mm and is made of concrete with a compressive strength of 26.9 MPa. It is reinforced with 10 longitudinal bars of Grade 380 (f_y = 432 MPa) with a diameter of 24 mm. The transverse reinforcement has a yield strength of 305 MPa and diameter of 12 mm placed at spacing of 80 mm. The clear cover to the transverse reinforcement is 24 mm. The column is under constant axial load of 646 kN while lateral cyclic load is applied on the top of the column. The specimen failed in a flexural mode where buckling of longitudinal reinforcement at the top displacement of 84 mm is reported. For the analytical simulation, the cross-section is divided into a number of fibers of confined as well as unconfined concrete incorporating material models of Hoshikuma *et al.* (1997) and Kent and Park (1971), respectively. For the steel fibers, two complete simulations using bi-linear as well as the proposed tri-linear model are performed and compared. The effect of buckling of longitudinal
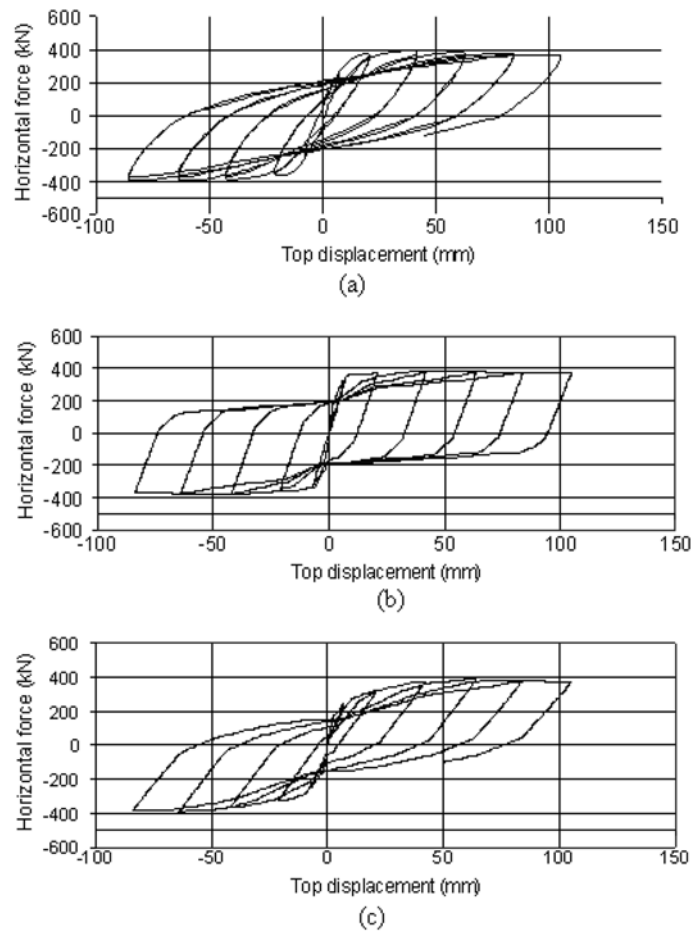

Fig. 7 Horizontal force-top displacement response for the column (a) experimental, (b) bilinear model, (c) tri-linear approximation

Table 1 Comparison of the maximum response for each cycle

Top Displacement (mm)	7	21	42	63	84	105
Experiment (kN)	257	340	365	374	373	368
Bilinear model (kN)	335	370	380	378	375	371
Tri-linear model (kN)	251	340	358	367	370	360

reinforcement corresponding to the maximum top displacement of 84 mm is simulated only in the tri-linear model. Fig. 7(a) illustrates the experimental results of the test in term of horizontal force vs. top displacement of the column. Figs. 7(b) and 7(c) show the analytical results of the test using steel material based on bilinear model, and the tri-linear approximation, respectively. It is observed that the tri-linear model is successful in yielding very comparable results to the experiment. Table 1 compares the maximum responses of the experimental test and the analytical simulations corresponding to a specific value of displacement at each cycle. Because the DRAIN-2DX analyses were performed for one cycle per drift level, the average value of the experimental test for each drift level for push and pull cycles is calculated and presented. It can be observed that the tri-linear model is more successful in simulating the test than the bilinear model especially with regards to the area enclosed by each hystersis loop which is representative of the dissipated energy through that cycle. The bilinear model overestimates the response of the initial cycles with small top displacements. The stiffness degradation and the values of plastic deformations at complete unloading where the curve crosses the axis of zero force are very comparable to the experimental observations.

5.4 Case-study 2

In this case study, the behavior of a cantilever circular column with spiral reinforcement tested by El-Bahy *et al.* (1999) is simulated. The column represents a bridge pier with a cross-section having a diameter of 305 mm and a height of 1372 mm. It is made of concrete with a compressive strength of 29 MPa, and is reinforced with 21 longitudinal bars with diameter of 9.5 mm with f_y = 448.5 MPa, and f_u = 690 MPa. Diameter of the spirals is 4 mm spaced at 19 mm with a yield stress of 434 MPa. The clear cover to the center of the hoop bar is 14.5 mm. The column is under constant axial load of 200 kN while lateral cyclic load is applied on top of the column. The specimen was subjected to three cycles, each at lateral displacement amplitudes of 1.0, 1.5, 2.0, 2.5, 3.0, 4.0, 5.0, and 6.0 percent until failure. It was reported that a smaller displacement cycle of 0.5 percent drift was applied between each drift level increase, to monitor the change in the specimen stiffness. Minor buckling and significant spalling was evident by the end of the 4.0 percent drift cycle. At the drift of approximately 5.5 percent the failure of the specimen was observed due to rupture of the spiral in the plastic hinge zone. Because of the size of the output data, only one cycle per drift level is performed for the computer simulation neglecting small displacement cycle of 0.5 percent drift. The material model for the confined and unconfined concrete based on Mander's model is used in this study incorporating the parameters based on the experimental values as reported in Kunnath (2004). The buckling of the outer rebars is simulated by the same procedure as described previously. However the rupture of the spirals before the failure could not be simulated as it compromises the assumption of the plane cross sections remain plane and it was believed to be the
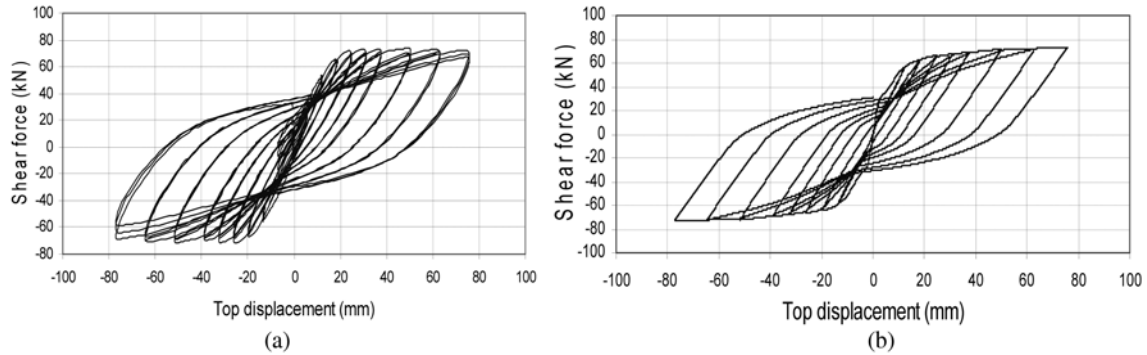
Fig. 8 Horizontal force-top displacement response for the column (a) experimental, (b) tri-linear approximation
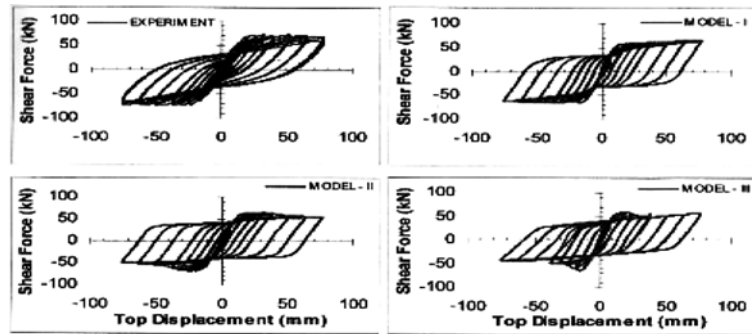

Fig. 9 Analytical results using fiber element (Kunnath 2004, with permission of ACI)

main reason for the difference between the experimental and analytical values of horizontal lateral force during the last cycles. Fig. 8 shows that the tri-linear model is successful in yielding comparable results to the experiment. The stiffness degradation and the value of plastic deformations at complete unloading where the curve crosses the axis of zero force are again very comparable to the experimental observations.

Kunnath (2004) used fiber section model implemented in the open source finite element software OpenSees (2004) to model the same test. Considering the low sensitivity of the result of that test to the confined concrete model, using different models with respect to yield strength and post-yield stiffness for steel behavior did not yield satisfactory results in terms of overestimation of the dissipated energy demonstrated by the enclosed area of the cyclic loops as can be observed from Fig. 9. It is believed that overestimation of the dissipated energy is somehow remedied by using the proposed tri-linear model for steel instead of the bi-linear one as can be observed from the results of case studies 1, and 2, in this paper.

5.5 Case-study 3

The ability of the model for simulating test of a cantilever column with circular cross-section and under variable axial load tested by Esmaeily and Xiao (1999) is evaluated. The RC column has a cross sectional diameter of 406.4 mm and a height of 1829 mm. It is made of concrete with the

compressive strength of 49.3 MPa, and is reinforced with 12 Grade 410 (f_y = 489.5 MPa, f_u = 579.2 MPa) 13 mm longitudinal bars. W2.5 at 32 mm is used for transverse reinforcement with a yield stress of 468.8 MPa. The clear cover to the transverse reinforcement is 13 mm. The column is under variable axial load of [tan (47.32º) × lateral force] while lateral cyclic load is applied on top of the column. The discretization of column's cross section into fibers of cover concrete, core concrete, and longitudinal steel is depicted in Fig. 10. There are four layers of rebar fibers in the cross section based on their distance to the mid-section as shown in Fig. 10. After defining the material models using the tri-linear approximation for steel behavior and the sectional properties of
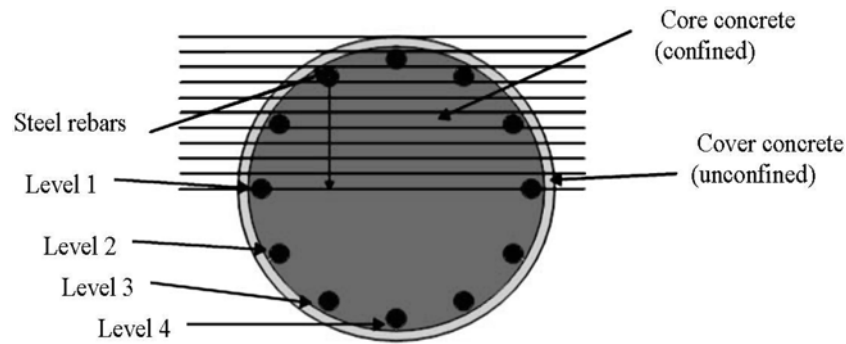

Fig. 10 Fiber discretization of cross section of the pier in Case-3
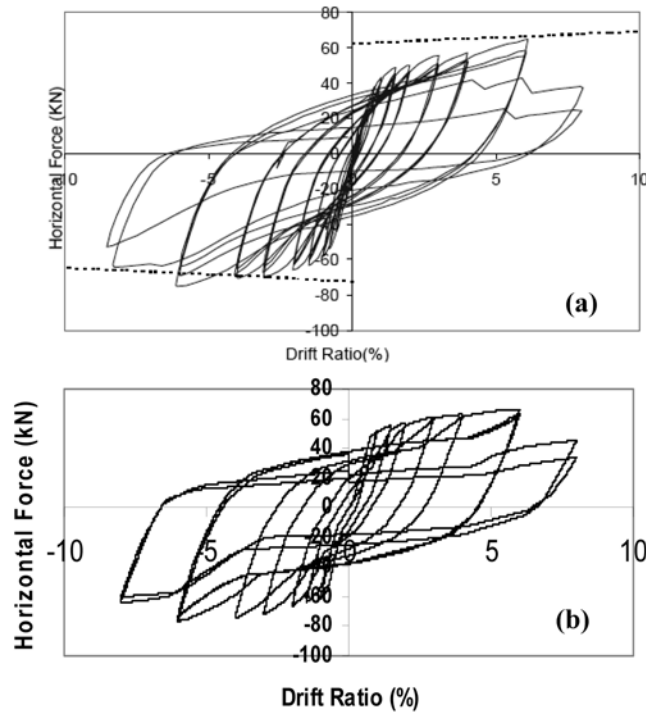

Fig. 11 Horizontal force-top displacement response (a) experimental (Esmaeily and Xiao 1999), (b) tri-linear model

fibers, a nodal load pattern consisting of a unit horizontal load, and vertical load of 1.08, representing tan 47.32° times the unit axial load, is defined in the program input data to be applied on the column's top throughout the entire analysis. This will ensure that the proportional axial force is applied simultaneously with the lateral load throughout the loading history. Comparison of the results as shown in Fig. 11 indicates a successful simulation of the analysis particularly before drift ratio of 6%. The axial force was proportional to the horizontal force and its value had opposite signs in two opposite directions. Therefore the cyclic behavior of the column was different in the pull and push directions. This difference is successfully captured in the analytical response as can be observed from comparison of the maximum responses in both directions in Fig. 11(b). The observation of the experimental test indicated that the furthermost rebar on the push side buckled at the second cycle of 6% drift ratio. The same behavior was observed on the opposite side of the column when the load reversal was applied. At the third cycle of 6% drift ratio, the two adjacent spirals ruptured followed by the buckling of the nearby rebars. The test was continued for the next step, at a drift ratio of 8%, at which the two buckled rebars ruptured. Simulation of the buckling behavior is done according to the procedure explained before. After running the analysis for first cycle at drift ratio of 6% based on stress-strain relationship values shown in Table 2, the maximum strains at the outmost concrete fibers were determined to be 0.081, and −0.012. Based on the strain gradient and the distance of the steel fibers to the end sections, the strain at outermost rebar level at onset of buckling was calculated as 0.074. This strain corresponds to stress of 573 MPa on the tri-linear curve. The stress strain values for the outermost rebar level are then modified as shown in the first two columns of Table 3. The stress-strain values in the last row show a very small increase in the stress level for a very large increase in the strain level (strain value is taken as a large arbitrary value of 1.0). This will ensure that the steel stiffness is very small after the buckling of the rebars. For the next cycle where buckling of adjacent rebars was reported, the same procedures as above are followed and the strain at the corresponding rebar level was calculated as 0.069, and the stress strain relationships for the rebars at level 3 are modified as shown in the last two columns of

Table 2 Tri-linear stress-strain relationships for steel at first cycle of drift ratio of 6%

Drift = 6%	Strains at rebar level (see Fig. 10)			
Stress (MPa)	Level 1	Level 2	Level 3	Level 4
391	.0065	.0066	.0066	.0067
513	.0261	.0265	.0266	.0267
580	.08	.08	.08	.08

Table 3 Modified tri-linear stress-strain relationships for steel at buckling

Level 4 at buckling (second cycle of 6% drift)		Level 3 at buckling (third cycle of 6% drift)	
Stress (MPa)	Strain	Stress (MPa)	Strain
391	.0067	391	0.0067
513	.0267	513	0.0269
573	.074	566	0.069
573.1	1.0	566.1	1.0

Table 3. For simulating the rupture of rebars, the corresponding steel fiber sections are removed from the beginning of the analysis of cycle of 8% drift ratio. The result is shown in Fig. 11(b) in which degraded loops are apparent at this level of drift.

6. Conclusions

This study shows that the fiber element incorporating the tri-linear approximation of reinforcing bar behavior and appropriate models for concrete, leads to very comparable analytical results to the experimental data. The steel tri-linear model yielded a better representation of the energy dissipation capacity and horizontal lateral force in comparison to conventional bilinear model. The validity of the fiber model is based on the assumption that plane sections remain plane and perpendicular to the longitudinal axis of the element throughout the deformation history. Therefore phenomena such as debonding and shear failure can not be implicitly accounted for. The model shows comparable results for several different experiments, three of which are presented in this paper. The analytical simulations of tests with high strength concrete which are not presented in this paper showed an abrupt softening of the response after the maximum strength was reached. The reason is believed to be the inappropriate representation of the descending branch of the monotonic behavior of concrete under cyclic loading as was pointed out earlier. Further studies are being conducted to model and evaluate the analytical results of cyclic loading behavior of high-strength concrete specimens. Results of a successful fiber element analysis, such as those presented in this paper, can be used for calibration of controlling parameters for a macro-model based analysis which facilitates the analysis of multi-member structures under seismic effect.

Acknowledgements

References

Allahabadi, R. and Powell, G.H. (1988), "DRAIN-2DX User Guide", Technical Report UCB/EERC 88/06, University of California, Berkeley.

Bae, S. and Bayrak, O. (2004), "Performance-based design of confining reinforcement: research and seismic design provisions", *International Symposium on Confined Concrete*, Changsha, China.

Bauschinger, J. (1887), "Variations in the elastic limit of iron and steel", *J. Iron Steel Inst.*, **12**(1), 442-444.

Bechtoula, H., Kono, S. and Watanebe, F. (2009), "Seismic performance of high strength reinforced concrete columns", *Struct. Eng. Mech.*, **31**(6), 697-716.

Dhakal, R.P. (2006), "Post-peak response analysis of SFRC columns including spalling and buckling", *Struct. Eng. Mech.*, **22**(3), 311-330.

Dodd, L. and Restrepo-Posada, J. (1995), "Model for predicting cyclic behavior of reinforcing steel", *J. Struct. Eng.*, **121**(3), 433-445.

El-Bahy, A., Kunnath, S.K., Stone, W.C. and Taylor, A.W. (1999), "Cumulative seismic damage of circular

bridge columns: Benchmark and low-cycle fatigue tests", *ACI Struct. J.*, **96**(4), 633-641.

Elwood, K.J. and Eberhard, M.O. (2006), "Effective stiffness of reinforced concrete columns", PEER Research Digest No. 2006-1.

Elwood, K.J. and Moehle, J.P. (2003), "Shake table tests and analytical studies on the gravity load collapse of reinforced concrete frames", PEER report 2003/01, Pacific Earthquake Engineering Research Center, Univ. of California, Berkeley, 346 pages.

Esmaeily-Gh, A. and Xiao, Y. (1999), "Behavior of reinforced concrete columns under variable axial loads", Report No. USC-SERP 99/01, Department of Civil Engineering University of Southern California, Los Angeles, California.

Filippou, F.C. and Issa, A. (1988), "Nonlinear analysis of reinforced concrete frames under cyclic load reversals", Rep. EERC 88/12, Earthquake Engineering Research Center, Univ. of California, Berkeley, California.

Furlong, R.W. (1979), "Concrete columns under biaxially eccentric thrust", *ACI J., Proceedings*, **76**(10).

Golafshani, A.A., Aval, S.B.B. and Saadeghvaziri, M.A. (2002), "The fiber element technique for analysis of concrete- filled steel tubes under cyclic loads", *Struct. Eng. Mech.*, **14**(2), 119-133.

Hoshikuma, J., Kawashima, K., Nagaya, K., and Taylor, A.W. (1997), "Stress-strain model for confined concrete in bridge piers", *J. Struct. Eng-ASCE*, **123**(5), 624-633.

Kent, D.C. and Park, R. (1971), "Flexural members with confined concrete", *J. Struct. Div.*, **97**(7), 1969-1990.

Krauberger, N., Saje, M., Planinc, I. and Bratina, S. (2007), "Exact buckling load of a restrained RC column", *Struct. Eng. Mech.*, **27**(3), 293-310.

Kunnath, S.K. (2004), "Influence of confinement modeling on cyclic response of reinforced concrete columns", *International Symposium on Confined Concrete*, Changsha, China.

Kwon, S.H., Zhao, Z. and Shah, S.P. (2008), "Effect of specimen size on fracture energy and softening curve of concrete: Part II. Inverse analysis and softening curve", *Cement Concrete Res.*, **38**(8-9), 1061-1069.

Lokuge, W.P., Sanjayan, J.G. and Setunge, S. (2004), "Constitutive model for confined high strength concrete subjected to cyclic loading", *J. Mater. Civil Eng.*, **16**, 297.

Lee, T.K. and Pan, A.D.E. (2001), "Analysis of composite beam-columns under lateral cyclic loading", *J. Struct. Eng-ASCE*, **127**(2), 186-193.

Lu, X.Z., Jiang, J.J. and Ye, L.P. (2006), "A composite crack model for concrete based on meshless method", *Struct. Eng. Mech.*, **23**(3), 217-232.

Maekawa, K., Pimanmas, A. and Okamura, H. (2003), *Nonlinear Mechanics of Reinforced Concrete*, Spon Press, New York, USA.

Mander, J.B. (1983), *Seismic Design of Bridge Piers*, Ph.D. Thesis, Dept. of Civ. Engrg., University of Canterbury, Christchurch, New Zealand.

Mander, J.B., Priestley, M.J.N. and Park, R. (1988), "Theoretical stress-strain behavior of confined concrete", *J. Struct. Eng-ASCE*, **114**(8), 1804-1826.

Mander, J.B., Priestley, M.J.N. and Park, R. (1988), "Observed stress-strain behavior of confined concrete", *J. Struct. Eng-ASCE*, **114**(8), 1827-1849.

Otani, S. (1980), "Nonlinear dynamic analysis of reinforced concrete building structures", *Can. J. Civil Eng.*, **7**(2).

Park, R. and Paulay, T. (1990), "Use of interlocking spirals for transverse reinforcement in bridge columns", Strength and Ductility of Concrete Substructures of Bridges, RRU (Road Research Unit) Bulletin, **84**(1), 77-92.

Paulay, T. and Priestly, M.J.N. (1992), *Seismic Design of Reinforced Concrete and Masonry Building*, Wiley, New York.

Ramamurthy, L.N. (1966), "Investigation of the ultimate strength of square and rectangular columns under biaxially eccentric loads", *ACI-SP*, **13**, 263-298.

Roesler, J., Paulino, G.H., Park, K. and Gaedicke, C. (2007), "Concrete fracture prediction using bilinear softening", *Cement Concrete Comp.*, **29**(4), 300-312.

Sakai, K. and Sheikh, S.A. (1989), "What do we know about confinement in reinforced concrete columns?" *ACI Struct. J.*, **86**(2), 192-207.

Shayanfar, M.A., Kheyroddin, A. and Mirza, M.S. (1997), "Finite element size effects in nonlinear analysis of

RC structures", *J. Comput. Struct.*, **62**(2), 339-352.

Shima, H., Chou, L. and Okamura, H. (1987), "Micro and macro models for bond behavior in reinforced concrete", *J. Fac. Eng. Univ. Tokyo*, **39**(2), 133-194.

Taucer, F.F., Spacone, E. and Filippou, F.C. (1991), "A fiber beam-column element for seismic response analysis of reinforced concrete structures", Report to the National Science Foundation and the California Department of Transportation, Earthquake Engineering Research Center, University of California, Berkeley, California.

Vebo, A. and Gali, A. (1977), "Moment-curvature relation of reinforced concrete slabs", *J. Struct. Div.*, **103**(3), 515-531.